Density functional study on a light-harvesting carotenoid-porphyrin-C_{60} molecular triad

Tunna Baruah[1], and Mark R. Pederson[2]
[1] *Department of Physics, University of Texas at El Paso, El Paso, TX, 79968 and*
[2] *Center for Computational Materials Science, Code 6392, Naval Research Laboratory, Washington DC 20375-5345*
(Dated: September 12, 2006)

We present a study on the electronic structure of a biology-inspired molecular triad which shows promises in replicating photosynthesis process in the laboratory. The triad contains three different units - C_{60}, porphyrin and beta-carotenoid. We present its geometrical and electronic structure, dipole moments, optical absorption spectrum and its polarizability calculated with an all-electron density functional approach. Such a study will be useful for further understanding of its photo-conversion properties.

PACS numbers:
Keywords: fullerene,light-harvesting,electronic structure,polarizability,absorption

I. INTRODUCTION

Biological light-harvesting systems, found mostly in plants and bacteria, show an impressive efficiency for solar energy conversion. The quantum efficiency of the light-harvesting process measured as the ratio of amount of energy converted to another form to the amount of energy absorbed, is more than 90% for the natural light-harvesting systems. On the other hand, the solar energy conversion devices based mostly on semiconductors have a much smaller efficiency. Therefore, bio-mimetic materials are currently widely studied to achieve efficient photovoltaic devices. The basic process in such devices, both man-made and natural, is the photo-induced charge separation process. Since the charge separation process will depend on the underlying nature of the electronic structure of the material, it is necessary to understand the electronic structure of the material first. Such an understanding of the energy levels is also necessary to manipulate the light absorption characteristics so that a broad absorption spectrum can be achieved. In this letter, we present our density functional theory (DFT) based study of geometrical and electronic structure along with optical and electrical properties of a biomimetic organic which shows photoinduced charge separation upon irradiation by a pulsed laser. This study forms the basis of further studies on the charge-separation process seen on this molecule.

The bio-inspired molecular photovoltaic that we are studying here was (see Fig. 1) first synthesized by Liddell *et al.* [1, 2] and contains three components - a diaryl base porphyrin, a beta-carotene molecule and a pyrrole-C_{60} molecule. The pyrrole ligand breaks the icosahedral symmetry of the C_{60} molecule and also connects it to the porphyrin. The porphyrin and the carotene are connected through an amide connector. The base porphyrin functions as a chromophore, the carotenoid as an electron donor and the C60 as an electron acceptor. The porphyrin molecule absorbs light in the red and blue (the so-called Q and Soret bands) region of the spectrum [3–5]. The change in absorption due to the presence of the hydrogens is small in that the main absorption peaks remain in the blue and red regions. The C_{60} molecule [6, 7],is known to accelerate photoinduced charge separation [8]. When the porphyrin is excited by absorption of light, the excited electron moves to the C_{60} which has an electron affinity of 2.7 eV. On the other hand, the beta-carotene also donates one electron to the excited porphyrin such that in the final state, the excited electron is on the C_{60} and the hole is on the beta-carotene. Thus the initial particle-hole pair created on the porphyrin separates and migrates in opposite directions similar to the charge separation of an exciton pair at a semiconductor junction. It may be mentioned here that there are several such molecules synthesized [9], however this molecule was chosen for our study mainly because there has been a number of studies performed on various aspects of this triad. Therefore, even though experimentally this molecule was not found to have a high quantum efficiency, we choose this molecule for our series of studies on organic photovoltaics. We point out that while some success in the DFT-based calculations of charge transfer energy has been achieved, this topic remains open and there is neither a rigorous theory nor numerically stable method for such calculations which is well developed or universally accepted. For a discussion see Refs 10–13. We are also engaged in development of a simplified approach to address the charge-transfer process in this molecule. Here, we are mainly focusing on the electronic structure of the molecule which also forms the basis of future work. These works will be published in future.

Gust et al. have observed that the the triad can be excited to a charge-separated state $C^{\cdot+}$-P-$C_{60}^{\cdot-}$ upon irradiation by laser at 590 nm with a quantum yield of 14% [1]. The experiments are carried out in solutions using different solvents. They found that the charge-separation process also depends on the nature of the solvent. While benzonitrile and 2-methyl-tetrahydrofuran as the solvent exhibited photo-induced charge separation, toluene on the other hand was shown to inhibit such processes. Thus

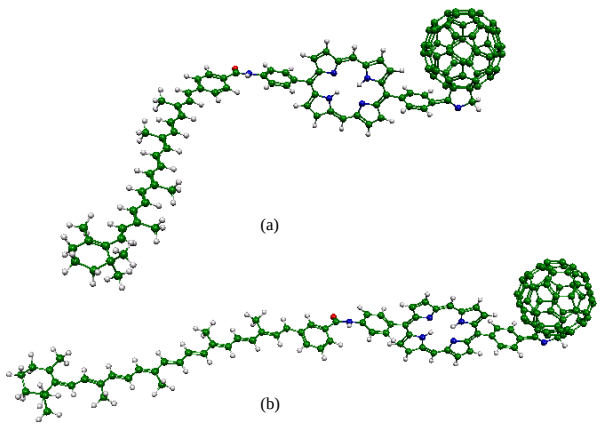

FIG. 1: The optimized structures of the elbow shaped and the linear geometries

it is obvious that the permanent dipole moment of the solvent molecules play an important role in the whole process. The charge-separated excited state of the triad molecule has a large dipole moment of 153 D [14]. The most likely effect of the solvent molecules would be stabilization of the large dipole state. It was recently shown that boolean operations can be performed using similar molecular triads [15]. Also, since it possesses a large dipole moment for the charge-separated state, it presents a possible molecular solar-cell component.

In the next section we present the computational details followed by the results and discussions in the subsequent section.

II. COMPUTATIONAL DETAILS

The electronic structure is calculated using density functional theory as implemented in the NRLMOL code [16–18]. The calculations are done at the all-electron level using a generalized gradient functional [19] to describe exchange and correlation between electrons. This is by far one of the largest ab-initio calculations where symmetry can not be exploited to reduce computational costs. The code uses a large gaussian basis set. The details of the basis set are summarized in Table II. A few salient points about the code are that the same set of primitive basis functions are used for all the contracted functions. The table also shows the range of the exponents (α) for the primitive gaussians. The NRLMOL code uses a mesh which is variational with respect to the accuracy of the integrals. The mesh size for this calculation is about 1.4

Atom type	Bare gaussians	contracted functions			Min α	Max α
		s	p	d		
H	6	4	3	0	7.7×10^{3}	7.4×10^{-3}
C	12	5	4	2	2.2×10^{6}	7.7×10^{-2}
N	13	5	4	2	5.2×10^{6}	9.4×10^{-2}
O	13	5	4	2	6.1×10^{6}	1.0×10^{-1}

TABLE I: The table shows the number of primitive gaussians used for each type of atoms, the minimum and maximum values of the exponents and the number of contracted gaussians.

million grid points. Another aspect of the code is that the Poisson equation is solved analytically leading to an accurate Coulomb potential. The code is also massively parallelized with very good scaling which makes it suitable for studying large molecular systems.

The geometry optimization was carried out using the LBFGS scheme [20, 21]. Initially the geometries of the separate units were optimized before constructing the triad. After forming the composite molecular triad, its geometry was optimized again. Since the molecule has a quite floppy structure, we optimized two different geometries. In the first geometry, the three subunits were attached such that the resultant triad has an elbow shape structure (see Fig. 1). Its energy after optimization turned out to be higher by about 0.6 eV and also the dipole moment for the final charge separated structure is much smaller. The linear geometry as shown in Fig. 1 was found to be lower in energy and all subsequent calculations were carried out on this geometry. In the optimization stage, the process was carried out until the smallest force was 0.003 eV/Å and RMS force was 0.076 eV/Å. It can be pointed out here that NMR studies on carotenoid-porphyrin dyad shows a structure similar to the linear structure [22]. Similar structure was found by Smirnov et al. as the lowest energy structure based on a molecular mechanics level calculation [23]. We would like to point out that the molecule has a long chain-like structure and can exhibit substantial temperature induced structural deformation. Since our study is aimed at understanding the zero-temperature state, such calculations are beyond the scope of present work.

The absorption spectra are calculated using the following expression which involves dipole matrix elements.

$$\sigma(E) = \int |<\psi_i|P|\psi_j>|^2 \, f_i(1-f_j)\delta(\epsilon_i - \epsilon_j - E) \quad (1)$$

Here P is the dipole operator and the ϵ_i are the single particle energy levels and $E = \hbar\omega$. f_i is the occupancy for the ith orbital. A reasonable broadening factor as discussed in Ref. [24] was used.

III. RESULTS AND DISCUSSION

The two optimized geometries of the triad, the elbow-shaped and the linear ones are shown in Fig. 1. As

mentioned earlier, all further calculations and hence discussions pertain to the linear molecule. The porphyrin unit is almost planar except for the hydrogen atoms at the center. The plane of the aryl ligands are at an angle of 90^o to the plane of the porphyrin. The C_{60} does not display much distortion from its icosahedral symmetry despite the presence of the pyrrole ligand. Gust et al. have found that replacing the diaryl-porphyrins with a tetraarylporphyrin can lead to an enhancement of the quantum yield [9]. The present molecule as shown in Fig.1 has a photoinduced charge separation efficiency of 14% whereas replacing the diarylporphyrin with tetraarylporphyrin increases it to 95%. However, calculations on the second structure is beyond the scope of the present work.

The density of states (DOS) for the triad is shown in Fig. 2. The bottom panel shows the DOS for the whole molecule and the upper three panels show the DOS projected onto the three subunits, namely, pyrrole-C_{60}, beta-carotenoid with the amide and the diaryl-porphyrin. Due to the large distances between the units, any significant hybridization of the molecular orbitals belonging to different components is not seen. The states are mostly localized on the parent components. The highest two occupied states (HOMO,HOMO-1) are localized on the β-carotene while the lowest three unoccupied states (LUMO, LUMO+1,LUMO+2) are localized on the C_{60}. The isolated fullerene molecule has a five-fold degenerate HOMO with H_u symmetry and a three-fold degenerate LUMO with T_{1u} symmetry [25]. The three LUMOs of the triad originate from the T_{1u} LUMO of the isolated C_{60}. However, the T_{1u} symmetry is broken here due to the lack of spherical symmetry. The energy gap between the highest occupied and the lowest unoccupied molecular orbitals (HOMO-LUMO) is 0.18 eV. The next two occupied levels (HOMO-2,HOMO-3), known as Gouterman orbitals, are from the diaryl-porphyrin complex. The band gap or the HOMO-LUMO gap as obtained from DFT does not reflect the correct energy required for transferring an electron from the β-carotene to the C_{60}. The actual excitation energy for the HOMO-LUMO transition can be estimated from the ionization potential (IP) of the β-carotene , the electron affinity (EA) of the C_{60} and including the particle-hole attractive Coulomb interaction. The excitation energy can be estimated as ($IP_{carotenoid}$ - EA_{C60} - 1/R). Such an estimate yields the HOMO-LUMO excitation energy at 2.5 eV which is much larger than the DFT HOMO-LUMO gap. Therefore, the DFT HOMO-LUMO separation energy can not be taken as the correct excitation energy for the charge-separation.

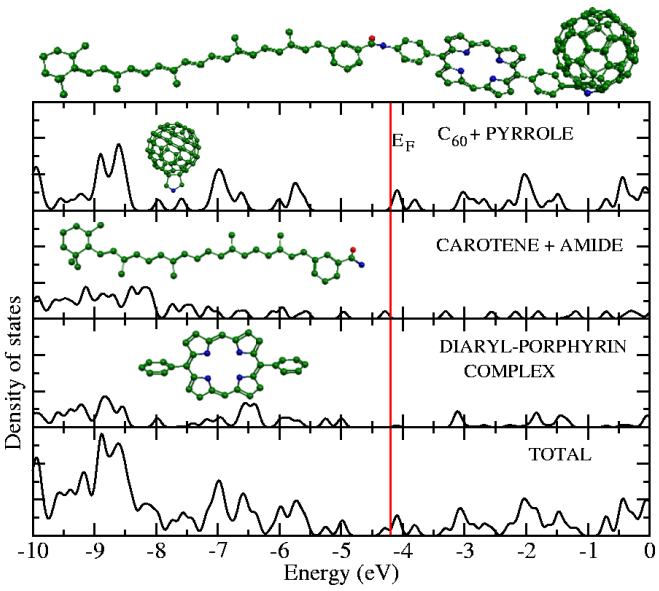

FIG. 2: The Gaussian broadened (FWHM = 0.005 a.u.) density of states projected onto the components of the triad are shown . The total DOS is shown in the bottom panel.

Although the charge-separation energies which involve excitation of electrons from orbitals of one component to orbitals of another component are not well reproduced in DFT calculations, the single-particle eigenvalues can still be used to obtain the localized excitations. The localized excitations are the ones where both the initial and final orbitals are located on the same component. As the overlap between the orbitals of different components are virtually zero, the absorption spectrum calculated using equation (1) yields the spectrum for localized excitations only.

The transient absorption spectra of the C-P-C_{60} triad in different solvents and at different temperatures were measured by Kuciauskas *et al.* [26]. Our calculated absorption spectra of the ground state of the triad and its components are shown in Fig. 3. The calculated spectrum can not be directly compared with the spectrum observed by Kuciauskas *et al.* since the transient spectrum is only the absorption spectrum of the excited state whereas our calculated spectrum is for the ground state. From the figure, it is apparent that the peaks of the spectrum for the triad can be assigned to transitions taking place on various components. The large peak at 1.0 eV occurs due to the transitions from HOMO to LUMO+3 both of which are localized on the carotenoid. There are other peaks due to transitions localized on the carotenoid, however, they are much smaller in intensity compared to the peak at 1 eV. It may be pointed out that water molecules also absorb energy at 1 eV and therefore excitation of the triad molecule at this frequency by solar radiation will be small due to the presence of atmospheric water vapor. The smaller peak at about 2.0 eV is the absorption peak of the Gouterman orbitals of isolated diaryl-porphyrin complex [3, 4]. This is the absorption line which is excited by pulse laser in the experiment showing photo-induced charge transfer. The other peak due to transitions located on the porphyrin is at about 5 eV. The peaks at about 3.0, 4.0 and 5.0 eV arises mostly from C_{60} transitions. These peaks are in good agreement with earlier published values for C_{60}, β-carotene and porphyrin [27–31]. As mentioned above, these are localized

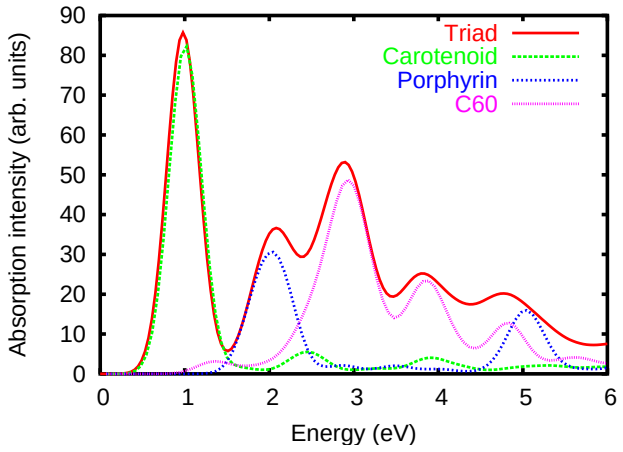

FIG. 3: The absorption spectrum of the triad. Peaks near 1 eV may be shielded by atmospheric water vapor.

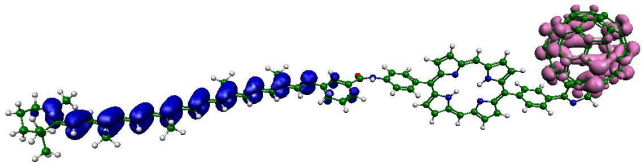

FIG. 4: An excited state where the particle orbital is on the C_{60} and the hole orbital is located on the β-carotene .

transition and therefore these transitions do not result in a large dipole change.

Gust et al. have observed that excitation by pulsed laser at 590 nm causes electronic transition on the porphyrin followed by a multistep electron-transfer process leading to the $C^{\cdot+}$-P-$C_{60}^{\cdot-}$state [1]. A charge-separated state with a large dipole moment of 153 Debye results since the largest molecular dimension is about 50 Å[14].

We have calculated the dipole moment for the ground state and estimated it for a number of excited states. The ground state of the molecule possesses a permanent dipole moment of 9.04 Debye. The dipole moment for the excited states were estimated as follows. We have chosen the highest 10 occupied and lowest 10 unoccupied states and from these 20 states in the transition region, constructed 100 singly excited states. The states that we have considered in this calculation are listed in table II. The dipole moments of the 100 excited states were calculated from the non-self-consistent excited state density $\rho_{ex} = \rho_g - \rho_h + \rho_p$ where g, h and p refer to the ground state total, hole and particle orbital densities. We find that the dipole moments of these singly excited particle-hole states lie between 5.8 to 180.3 D. The calculated dipole moment is overestimated since the electron densities for these states are only approximate. Also for the C_{60} unoccupied orbitals, the final particle orbital could well be a linear combination of the three lowest unoccupied orbitals. Despite the approximate nature of our calculation for excited state dipole moments, it can be stressed that the dipole moments for this molecule would be large due its sheer size. We show one such state with a large dipole moment in Fig. 4. In this figure, the densities of the particle (on C_{60}) and hole (on β-carotene) orbitals are depicted. We find that quite a few excited states have a large dipole moments where the occupied orbital or the particle is localized either on the C_{60} or on the β-carotene and similarly the hole is localized either on the β-carotene or on the C_{60}. The other charge separated states such as C-P^+-C_{60}^- have comparatively smaller dipole moments of about 70 D due to the smaller particle-hole separation. Nevertheless, the dipole moments for excitations involving orbitals from two different components are in general large.

TABLE II: Eigenvalues (eV) and molecular parentage of the ten highest occupied and ten lowest unoccupied orbitals (-ϵ_{Fermi}=4.29 eV).

Hole			Particle		
Index	$-\epsilon$	Parentage	Index	$-\epsilon$	Parentage
1	5.77	C_{60}	11	4.11	C_{60}
2	5.76	C_{60}	12	4.08	C_{60}
3	5.69	C_{60}	13	3.81	C_{60}
4	5.69	Porphyrin	14	3.31	Carotene
5	5.60	C_{60}	15	3.13	Porphyrin
6	5.56	Carotene	16	3.09	Porphyrin
7	5.25	Porphyrin	17	3.05	C_{60}
8	5.00	Porphyrin	18	2.99	C_{60}
9	4.96	Carotene	19	2.85	C_{60}
10	4.29	Carotene	20	2.68	C_{60}

We have also calculated the polarizability of this molecule by self-consistently calculating the dipole moments for different values of applied electric field along three perpendicular directions. The polarizabilities were calculated from these values using a finite difference method [25, 32]. The mean polarizability of the molecule is 549.4 $Å^3$ with a large polarizability component along the molecular axis. The mean polarizabilities of carotene, porphyrin, and C_{60} components are 208.5, 81.1 and 96.8 $Å^3$, respectively. The polarizabilities of the β-carotene and the triad along the primary axis is however much larger. The large values of polarizability can also be attributed to the delocalized states on the β-carotene and the effective fields due to the induced dipoles on the components leading to a large polarizability component for the composite molecule.

In conclusion, our DFT calculations have shown that for the linear molecule, the hybridization between or-

bitals of different component is negligible. Because of the small overlap, the absorption spectrum of the triad is somewhat similar to a linear combination of the spectra of the components. The calculated spectrum shows peaks for the components which are in good agreement with earlier published results. These transitions are localized and do not lead to large dipole moment states. We have estimated the dipole moments for 100 excited states and our calculations show that this molecule in the charge-separated state can have a large dipole moment. Our estimation shows a dipole moment of 180.3 D for the charge-separated state. We also find that the molecule has very large polarizability.

Our calculations also show that Kohn-Sham density functional theory can not treat the particle-hole excited states correctly. We find the excitation energy for the charge-separation to be drastically underestimated. Therefore application of DFT for charge-separation requires further development for better description of excited states. While excited states are not formally accounted for in DFT, we believe a simple extension would be sufficient for singly excited states. It is well-known that ΔSCF method can yield pretty good excited state energies though it lacks rigorous justification. While this method is applicable to most systems, for charge transfer cases, e.g. dissociation of NaCl molecule, it is not useful due to numerical difficulties such as charge-sloshing. A method that can circumvent the charge-sloshing problem can still yield reliable results for singly excited states. However, in Δ-SCF method, the excited states are not orthogonal to the ground state and hence can lead to lower energies. On the other hand, the advantage of relaxation of the orbitals in the new Coulomb potential is not to be underestimated. Our future calculations on this molecule will be directed towards this goal.

Authors acknowledge ONR (Grant No. N000140211046) and DoD CHSSI Program. TB acknowledges NSF Grants No. HRD-0317607 and NIRT-0304122. This work was performed in entirety on the SGI-Altix system at NRL-DC under the auspices of the DoD HPCMP. Authors thank CCS, NRL, especially W. L. Anderson and J. E. Osburn, for providing computational resources.

[1] P.A. Liddell, D. Kuciauskas, J. P. Sumida, B. Nash, D. Nguyen, A.L. Moore, T. A. Moore, D. Gust, J. Am. Chem. Soc. **119**, 1400 (1997).
[2] D. Carbonera, M. D. Valentin, C. Corvaja, G. Agostini, G. Giacometti, P. A. Liddell, D. Kuciauskas, A. L. Moore, T. A. Moore, D. Gust, J. Am. Chem. Soc. **120**, 4398 (1998).
[3] M. Gouterman, J. Mol. Spectros. **6**, 138 (1961).
[4] R. Husánk and O. Horváth, Chem. Comm., 224 (2005).
[5] G. Knör, Inorg. Chem. Comm. **4**, 160 (2001).
[6] H. W. Kroto *et al.* , Nature (London) **318**, 162 (1985).
[7] W. Kratschmer *et al.* , Nature (London) **347**, 254 (1990).
[8] N. S. Sariciftci, L. Smilowitz, A. J. Heeger, F. Wudl, Science **258**, 1474 (1992).
[9] G. Kodis, P. A. Liddell, A. L. Moore, T. A. Moore, and D. Gust, J. Phys. Org. Chem. **17**, 724 (2004).
[10] W. G. Han, T. Lovell, T. Liu, L. Nooodleman, ChemPhysChem, **3**, 167 (2002).
[11] F. R. Salisbury, W. G. Han, L. Noodleman, C. L. Brooks, ChemPhysChem, **4**, 848 (2003).
[12] A. Dreuw and M. head-Gordon, J. Am. Chem. Soc. **126**, 4007 (2004).
[13] M. E. Casida, F. Gutierrez, J. Guan, F. X. Gadec, D. Salahub, J. P. Daudey, J. Chem. Phys. **113**, 7062 (2000).
[14] S. N. Smirnov, P. A. Liddell, I. V. Vlassioul, A. Teslja, D. Kiciauskas, C. L. Braun, A. L. Moore, T. A. Moore, and D. Gust, J. Phys. Chem. A **107**, 7567 (2003).
[15] J. Andreasson, G. Kodis, Y. Terazono, P. A. Liddell, S. Bandyopadhyay, R. H. Mitchell, T. A. Moore, A. L. Moore, D. Gust, J. Am. Chem. Soc. **126**, 15926 (2004).
[16] M. R. Pederson and K. A. Jackson, Phys. Rev. B. **41**, 7453 (1990).
[17] M. R. Pederson and K. A. Jackson, Phys. Rev. B. **43**, 7312 (1991).
[18] K. A. Jackson and M. R. Pederson, *ibid* **42**, 3276 (1990).
[19] J. P. Perdew, K. Burke and M. Ernzerhof, Phys. Rev. Lett. **77** , 3865 (1996).
[20] D. C. Liu and J. Nocedal, Math. Programming **45**, 503 (1989).
[21] J. Nocedal, Math. Comp. **24**, 773 (1980).
[22] D. Gust, T. A. Moore, A. L. Moore, C. Devadoss, P. A. Liddell, R. M. Hermant, R. M. Nieman, L. J. Demanche, J. M. DeGranziano, I. Gouni, J. Am. Chem. Soc. **114**, 3590 (1992).
[23] S. N. Smirnov, P. A. Liddell, I. V. Vlassiouk, A. Teslja, D. Kaciauskas, C. L. Braun, A. L. Moore, T. A. Moore, and D. Gust, J. Phys. Chem. A **107**, 7567 (2003).
[24] W. Y. Ching, Y. N. Xu, and K. W. Wong, Phys. Rev. B **40**, 7684 (1989).
[25] M. R. Pederson and A.A. Quong, Phys. Rev. B **46**, 13584 (1992).
[26] D. Kuciauskas, P. A. Liddell, S. Lin, S. G. Stone, A. L. Moore, T. A. Moore, and D. Gust, J. Phys. Chem. B **104**, 4307 (2000).
[27] J. R. Heath, R. F. Curl, and R. E. Smalley, J. Chem. Phys. **87**, 4236 (1987).
[28] Q. Gong, Y. Sun, Z. Huang, X. Zhu, Z. N. Gu, and D. Qiang, J. Phys. B: At. Mol. Opt. Phys. **27**, L199 (1994).
[29] L. Edwards, D. H. Dolphin, M. Gouterman, and A. D. Adler, J. Mol. Spectrosc. **38**, 16 (1971).
[30] M. Rubio, B. O. Roos,L. Serrano-Andres, and M. Merchan, J. Chem. Phys. bf 110, 7202 (1999).
[31] T. Polivka and V. Sundström, Chem. Rev. **104**, 2021 (2004) and the references therein.
[32] R. R. Zope, T. Baruah, M. R. Pederson, and B. I. Dunlap, to be published.